

OPEN ACCESS

The microstructure of Si surface layers after He⁺ Ar⁺ plasma immersion ion implantation

To cite this article: J M Chesnokov *et al* 2013 *J. Phys.: Conf. Ser.* **471** 012049

View the [article online](#) for updates and enhancements.

You may also like

- [Methods to improve antibacterial properties of PEEK: A review](#)
Idil Uysal, Ayen Tezcaner and Zafer Evis
- [Investigation of structural and optical properties of near surface of CdTe film induced by nitrogen plasma immersion ion implantation](#)
E R Shaaban, A E Metawa, A Almomhammedi *et al.*
- [A Comparison of Dry Plasma and Wet Chemical Etching of GaSb Photodiodes](#)
Vinay Bhagwat, J. P. Langer, Ishwara Bhat *et al.*



ECS
The
Electrochemical
Society
Advancing solid state &
electrochemical science & technology

DISCOVER
how sustainability
intersects with
electrochemistry & solid
state science research

The microstructure of Si surface layers after He⁺ and Ar⁺ plasma immersion ion implantation

J M Chesnokov¹, A L Vasiliev^{1,2}, V F Lukichev³ and K V Rudenko³

¹ National Research Centre “Kurchatov Institute”, Moscow, Russia

² Institute of Crystallography Russian Academy of Sciences, Moscow, Russia

³ Institute of Physics and Technology Russian Academy of Sciences, Moscow, Russia

E-mail: a.vasiliev56@gmail.com

Abstract. Processes accompanying the amorphization of Si surface layer after Ar⁺ and He⁺ low energy plasma immersion ion implantation were studied by transmission electron microscopy and microanalysis. The ion energies varied in the range of 0.5 – 3 keV with the doses of 5·10¹⁵ cm⁻² for Ar⁺ and 2·10¹⁶ cm⁻² for He⁺ pre-amorphization implants. A perturbation of Si lattice together with porosity was found. The utilization of heavy and light ions causes distinctive microstructural peculiarities. The presence of oxygen and its distribution near the surface layer was determined by electron energy loss spectroscopy.

1. Introduction

The downscaling of design rules for ultra-large scale integration circuits (ULSI) to sub-32 nm requires manufacturing extremely highly doped and thin source and drain regions of integrated Si MOSFETs. The thickness of doped Si layer should not exceed 10-15 nm. New technology of doping – the plasma immersion ion implantation (PIII) is a promising technique for that purposes [1]. Most difficulties appear with p-type of doping where B has no alternatives due to high solubility threshold in Si. However, the small B atoms implanted in Si undergo well-known channeling effect and to prevent this, the preliminary amorphization of thin Si layer is required. Conventional pre-amorphizing implants (PAI) are Si⁺ or non-active ions like Ar⁺ or other inert gases. The use of heavy ions and high dose PAI results in the surface sputtering together with Si amorphization. The sputtering is very critical for shallow junctions [2]: the surface recess limits for sub-32 nm MOSFETS is about 1 nm.

Therefore, the PAI processes of Si with light ions, especially with He⁺, is of great interest and has been extensively studied recently [3, 4]. The mechanisms of the amorphization and sputtering of solids by high energy ions are different for heavy and light ions [5]. The microstructure of amorphous layers could be different as well. That could cause peculiarities in diffusion and electrical activation behaviour of B dopant during rapid thermal annealing (RTA) process of implanted Si layers. The anomalous transient retrograde diffusion of B in Si during RTA after PIII-process with He⁺ PAI found in [6] was not observed in Ar⁺ PAI [7]. It was proposed that specific defects of an amorphous silicon layer caused by He⁺ implantation and its behaviour during subsequent annealing was responsible for difference in B diffusion [6]. However, no systematic research of the Ar⁺ and He⁺ implanted Si with low ion energy $E < 3$ keV was done. In this study a thorough analysis of the microstructure of Si after 0.5-3 keV Ar⁺ and He⁺ PAI was performed.



2. Experiment.

Ions of He⁺ and Ar⁺ were implanted in wafers of n-type Si(100) (4.5 Ohm-cm). The implantation process was carried out using experimental setup in plasma immersion mode by switching the wafer on negative square shaped pulsed accelerating potential with duration of 10 μsec. The repetition rate of accelerating pulses was 1 kHz. The ion current density measured during pulses of implantation was in the range of 10 – 20 mA/cm². The wafer was placed on a water cooled chuck with helium feeding between the chuck and the sample to prevent overheating and the wafer temperatures at implantation process did not exceed 100°C. The experimental conditions for all samples are described in Table 1.

Table 1: The ion energies and the exposure dose used.

	Group I – Ar ⁺ PAI			Group II – He ⁺ PAI		
Sample #	1	2	3	4	5	6
Energy, keV	0.5	1	3	0.5	1	3
Dose, cm ⁻²	5 x 10 ¹⁵	5 x 10 ¹⁵	5 x 10 ¹⁵	2 x 10 ¹⁶	2 x 10 ¹⁶	2 x 10 ¹⁶

The cross-sections of all samples for TEM were prepared by conventional way: mechanical thinning of glued slabs to the thickness of 10-20 μm followed by ion milling in Gatan PIPS (Gatan, USA) by Ar⁺ ions at an angle of 6° and an energy of 4 keV from the both sides of the sample. After the perforation of the sample the final cleaning with Ar⁺ ions with an energy of 100 eV was carried out for 5 minutes.

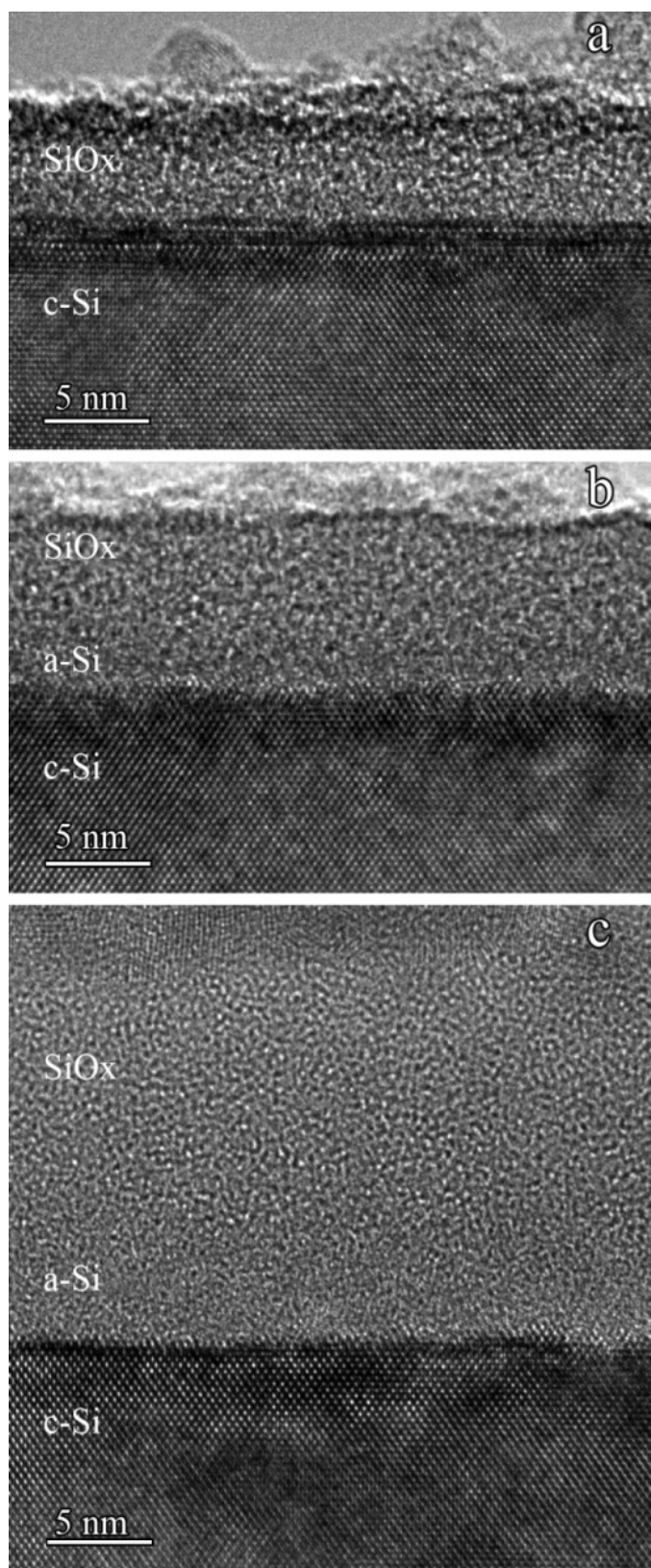
The microstructural study was performed in a Titan 80-300 TEM/STEM (FEI, USA) with an accelerating voltage of 300 kV. The electron microscope was equipped with probe C_s corrector, high angle annular dark field detector (HAADF, Fischione, USA), Gatan image filter (GIF) and windowless energy dispersive X-ray spectrometer (EDXS, EDAX, USA). The bright field (BF) TEM, high resolution (HRTEM) and HAADF STEM operation modes together with 3-window elemental mapping technique were used in our investigations.

3. Results and discussion.

3.1. The microstructure of Si after Ar⁺ PAI.

The BF HRTEM images obtained from cross-sectional specimens after Ar⁺ PAI at $E_{Ar} = 0.5$ keV, 1 keV, 3 keV are presented in Figure 1 (a-c) correspondingly. Several layers having different contrast were found and their presence and thickness depended on ion energy. One or two amorphous layers were observed near the specimen surface. They could be resolved by slightly different contrast and Fast Fourier Transform (FFT) power spectra which were obtained from these parts of the image to prove the difference. Energy filtering (EF) of the images was used to determine O distribution in the amorphous layers. The sample surface after Ar⁺ PAI with $E_{Ar} = 0.5$ keV looked wavy and the amorphous layer thickness determined from HREM image was 5±1 nm. The thickness of the layer was close to native SiO_x (3-5 nm) with similarly cleaned (001) Si surface. In that sample no difference in the contrast across the amorphous layer was observed and the small thickness of the layer prohibited the application of FFT analysis. The EF indicated that O was present in the amorphous layer from the top to the bottom of the layer. The attempts to obtain distinct Ar distribution failed and that could be due to additional Ar⁺ implantation during Ar⁺ milling of the sample. Below SiO_x/Si interface there was a crystalline layer exhibiting darker contrast, probably due to the presence of Ar⁺ ions in the end of range. The bottom interface of that area was not flat and displayed faceting parallel to {111} Si planes. Close inspection of Si crystal planes in the adjacent area demonstrated distortion of planes, however, defects like dislocations or stacking faults were not found.

The HRTEM image of the sample after Ar⁺ PAI at $E_{Ar}=1$ keV is shown in Figure 1 b. The overall thickness of the amorphous layer was 8 nm. The surface of the sample was not flat revealing an unevenness up to 1 nm height. The EF imaging indicated that 6-7 nm thick SiO_x layer was formed near the surface and the adjacent a-Si layer was about 1-2 nm. The crystalline Si (c-Si) surface was wavy with unevenness height of 0.5-1 nm. Again, the layer exhibiting darker contrast was below the a-Si/c-



Si interface and defects were found in the wavy (top) part which could be due to the overlapping of a-Si and c-Si.

The amorphous layer in the sample after Ar⁺ PAI at $E_{Ar}=3$ keV was 17 nm thick (Figure 1 c) and, according to the EF data, the top part was O enriched. The thickness of that SiO_x layer was 8-11 nm, which is much thicker than typical native SiO₂. The FFT spectra analysis demonstrated a single maximum for the SiO_x layer and double maxima for the a-Si layer with peak positions close to the previous sample. The upper layers of c-Si had a microstructure similar to the sample after PAI at $E_{Ar}=1$ keV. The study of the reason for the formation of this SiO₂ layer is on the way.

3.2. The microstructure of Si after He⁺ PAI

After He⁺ PAI with $E_{He}=0.5$ keV only one amorphous layer with thickness of 2 nm was observed (Figure 2 a). According to the EF study, the layer contained O. On several images we found a visibly distorted layer (0.5 nm) on the top of c-Si.

Increasing the He⁺ ions energy to 1 keV resulted in severe changes of overall microstructure. Three amorphous layers were found on the Si surface and they are shown in Figure 2 b:

1. a-SiO_x layer with thickness of 5-6 nm. The thickness of the layer was determined with the EF imaging.
2. a-Si layer. The thickness of the layer was estimated from BF and HAADF images and was 5-6 nm.
3. 10 nm thick a-Si layer with pores. The pore dimensions were up to 10 nm.
4. c-Si with high density of structural defects. HREM study revealed terminated crystal planes and black-white contrast typical for dislocations. The dark contrast on HAADF images indicated the presence of smaller pores (< 4 nm) in the top part of the layer. Bottom part of the layer exhibited darker contrast in HREM image (Fig. 2 b), probably due to absence of pores.

Figure 1. Cross-sectional BF TEM images of Ar⁺ PAI sample with energies of 0.5 (a), 1 (b) and 3 keV (c).

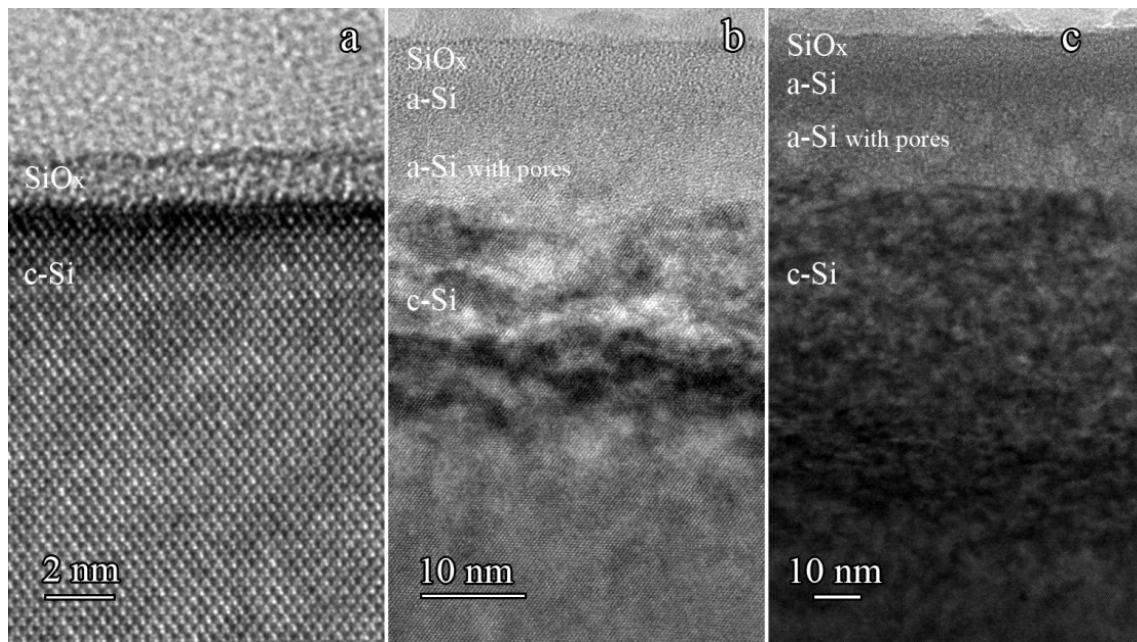


Figure 2. Cross-sectional BF TEM images of He⁺ PAI sample with energies of 0.5 (a), 1 (b) and 3 keV (c).

These pores could be the consequence of helium bubbles formed in the upper layers. After He⁺ PAI with $E_{\text{He}}=3$ keV the number of the layers and their morphology were similar to the He⁺ PAI at $E_{\text{He}}=1$ keV. The thickness of a-SiO_x was 7 nm and that of a-Si 5-6 nm. The larger pores (up to 10 nm) were in the a-Si layer and smaller (<6 nm) in the c-Si. Again, the pore density was much higher in the top part of c-Si layer and that area appeared brighter in the HREM image (Figure 2 c).

4. Conclusion

Different microstructure was found near Si surface after Ar⁺ and He⁺ low energy plasma immersion ion implantation. The Ar⁺ PAI results in formation of only amorphous layers while He⁺ PAI leads to the amorphous together with highly defective crystalline layer formation. The presence of oxygen and its distribution near the surface layer was determined by electron energy loss spectroscopy.

References

- [1] Anders A 2000 *Handbook of Plasma Immersion Ion Implantation and Deposition*. New-York, John Wiley & Sons.
- [2] International Technology Roadmap for Semiconductors. 2011 Edition (online at <http://www.itrs.net/Links/2011ITRS/Home2011.htm>).
- [3] Sasaki Y, Jin CG, Tamura H and Mizuno B 2004 *Proc. IEEE Symposium on VLSI Technology*, 180.
- [4] Mizuno B 2008 *Electronic Device Architectures for the Nano-CMOS Era*, Pan Stanford Publ. 141.
- [5] Falcone G 1990 *La Revista del Nuovo Cimento*. **13** 1.
- [6] Lukichev V, Rudenko K, Orlikovsky A, Pustovit A and Vyatkin A 2008 *17th Int. Conf. on Ion Implantation Technol. AIP Conference Proceedings*. **1066** 481.
- [7] Rudenko K, Averkin S, Lukichev V, Orlikovsky A, Pustovit A and Vyatkin A 2006 *Proc. SPIE* **6260** 626003.